Efficiency of Chain-CVTs at Constant and Variable Ratio

A new mathematical model for a very fast calculation of chain forces, clamping forces, clamping ratio, slip, and efficiency

Peter Tenberge
Institute of Design and Driving Engineering, Chemnitz University of Technology

ABSTRACT

The efficiency of chain-CVTs depends on friction forces and slip between the chain and the pulleys. The slip itself results from the elastic deformations of the pulleys, shafts, and the chain and from additional motions between chain and pulleys when changing the transmission ratio. The local friction forces depend on the local axial clamping forces and the local friction coefficients. A new mathematical model has been developed to calculate these relationships even in conditions with variable transmission ratio and furthermore with a very high calculation speed. Additional results are the relations between the clamping forces, which are necessary to transmit a certain torque at a certain ratio and a particular adjusting-speed, and the efficiency as well as the safety from gross slip. With this new tool it is much easier to improve the design of the CVT as well as the hydraulic system and the control strategies resulting in higher torque capacities and reduced power losses.
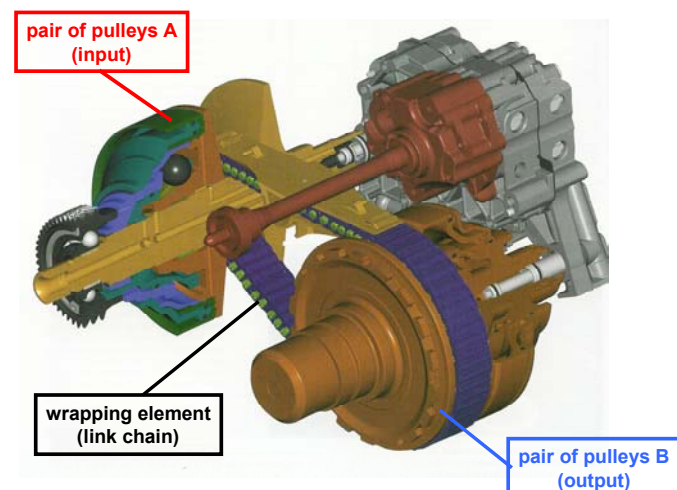
Fig. 1: Variator (pulleys, chain, hydraulic system) from Audis „multitronic"-CVT

INTRODUCTION

According to Figures 1 and 2, a continuously variable chain or belt CVT consists of a first pair of pulleys A and a second pair of pulleys B, each having a fixed pulley and a pulley movable in axial direction as well as a chain or a belt that is wrapped around these pulleys. The following considerations apply in particular to gears with wrapping elements like push belts or link chains, that is to say with a finite number of contacts to the pulleys.
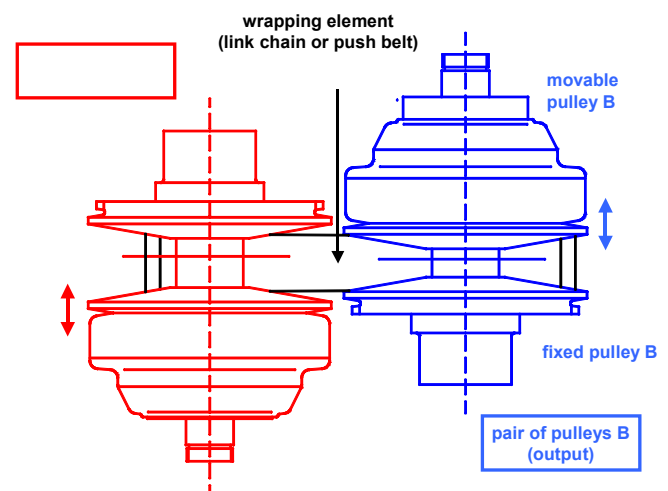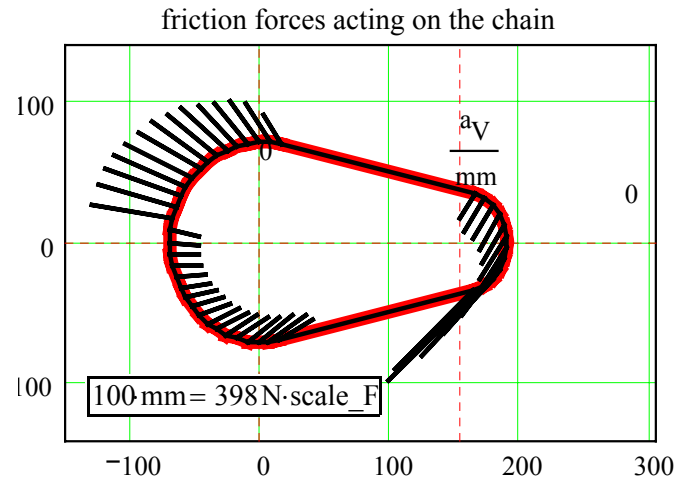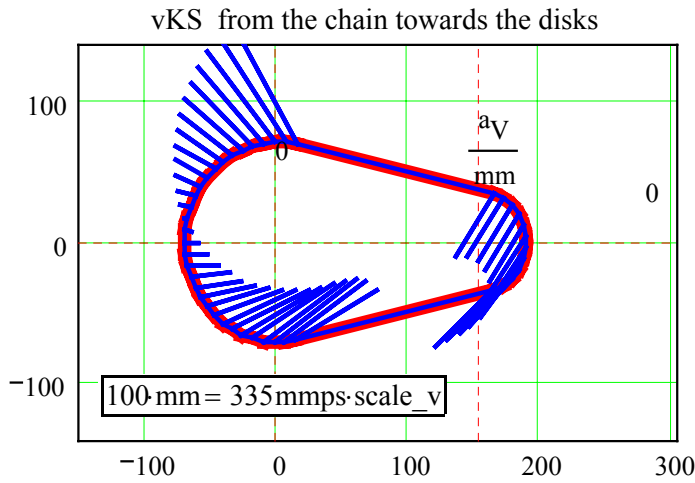

Fig. 2: Schematic structure of a continuously variable wrap gear

In such a CVT the torque is transmitted through friction forces in lubricated contacts between the chain and the cone pulleys. In this case the friction coefficients are in a range between $0.07<\mu<0.11$, depending on lubricant and surface roughness. Thus, very high contact normal forces are necessary for a high torque capacity. These high contact normal forces deform the pins of the chain links as well as the pulleys, which should remain light-

vKS from the chain towards the disks

$\dfrac{a_V}{mm}$

0

0

$100 \cdot mm = 335\,mmps \cdot scale\_v$

−100

−100   0   100   200   300

friction forces acting on the chain

$\dfrac{a_V}{mm}$

0

0

$100 \cdot mm = 398\,N \cdot scale\_F$

100

−100   0   100   200   300

stiffness = "normal"

$iV = 0.5$ $vK = 14.72\dfrac{m}{s}$

$r_A = 70.3\,mm$ $nA = 2000\,min^{-1}$

$r_B = 35.1\,mm$ $nB = 3984\,min^{-1}$

$diVdt = -0.52\dfrac{1}{s}$ $drAdt = 20\dfrac{mm}{s}$

$drBdt = -27\dfrac{mm}{s}$

$TA = 250\,Nm$ $Pan = 52.4\,kW$

$Fu = 3558\,N$ $\eta_{KS} = 95.86\%$

$FF = 260\,N$ $\mu_{max} = 0.09$

$Fmax = 6224\,N$ $PVA = 1330\,W$

$Fmin = 2666\,N$ $PVB = 839.5\,W$

$\varepsilon = 2.335$ $SA = 48.7\,kN$

$\zeta = 1.901$ $SB = 25.6\,kN$

input A   output B

450
360
270
180
90
0
−90
−180
−270
−360
−450

180

γ [°]

180

r-r$_m$ [μm]

0   10   20   30   40

bolt-Nr. on the wrap curve

input A   output B

8

$\dfrac{Fmax}{kN}$

X

F [kN]

$\dfrac{Fmin}{kN}$

6

4

2

ΔS [kN]

0

0   10   20   30   40

bolt-Nr. on the wrap curve
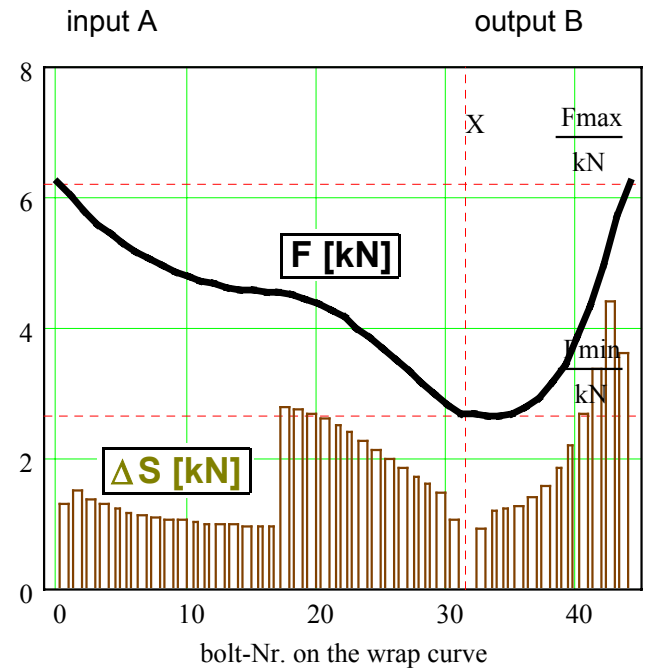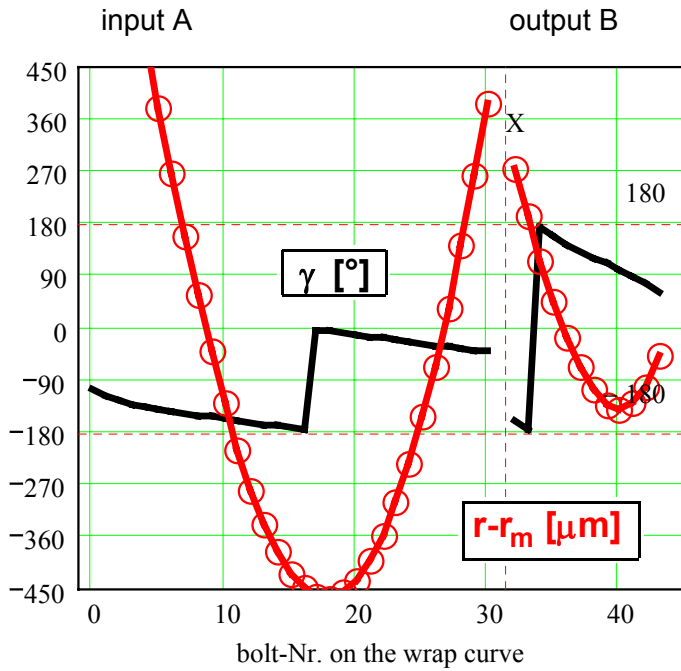
Fig. 3:   Operating point with variable ratio:

iV=0.5, diV/dt=-0.52 Hz,
TA=250 Nm, nA=2000/min, ε=2.331, SB=25.7 kN

weight with regard to the gear weight. Due to these deformations, the chain does not wrap around the pulleys on a circular arc, but moves around the pulleys with additional radial motions inwards or outwards.

To these sliding movements in radial direction a circumferential slip is added, which arises from the longitudinal elasticity of the chain and the changes of the contact radii due to the radial movements. Beside this, there are some more sliding movements if the ratio is changed.

All sliding movements add up to a total slip between the chain and the pulleys. The local friction forces counteract the local sliding movements and cause the change of forces within the chain and thereby they transmit the torque through the gear.

For an exemplary operating state with a variable ratio, Figure 3 illustrates true to the scale the local sliding speeds vKS of the chain towards the pulleys, the local frictional forces R, the local contact radii r of the chain pins in comparison to the average contact radius r_m, the sliding angles γ which result from the overlay of all components of the sliding speeds, the course of the chain forces F, and the local clamping forces ΔS.

Such relationships for stationary operating states are known very well for a long time from measurements and theoretical studies [1-9]. However, the today available calculation algorithms [7, 8] require long CPU times for the analysis of an operating point and can often be operated only by experts. Up to now, a simple tool is missing to support development processes with which these parameters can be computed for stationary and for transient operating states in a sufficiently exact, fast and easy way. For this purpose, a new calculation approach is presented in this paper.

GEAR DATA

The power transmission in continuously variable chain gears shall be explained exemplarily at a gear with the following data.

Data of the variator:

Center distance:	a_V = 155 mm
Maximum radius of contact:	r_{max} = 74 mm
Stiffness of the pulleys:	normal
Guidance length of the movable pulley:	gl_{mp} = 68 mm
Guidance clearance of the movable pulley:	gc_{mp} = 20 μm
Radius of curvature of the pulleys:	$r_{curvature}$ = 1653 mm
Distance between the center of the curvature of the pulleys and the axis:	r_W = 234 mm

Data of the chain:

Length:	L_K = 649 mm
Width:	b_K = 24 mm
Mass:	m_K = 0,778 kg
Number of links:	z_{KE} = 78
Pitch:	T_K = 8,321 mm
Longitudinal elasticity:	cl_K = 324,5 μm/N
Cross-elasticity (at each pair of pins):	cq_K = 5,714 μm/N

Friction coefficient:

Maximum friction coefficient between chain and pulley:	μ_{max} = 0,09

The friction coefficients can either be assumed as being constant or as variable according to friction-laws that are free to define. These friction-laws result from the comparison of calculated results and experimental studies. According to previous studies, with constant friction coefficients that are equal on both pulleys good correspondence with test results was achieved.

SLIDING MOVEMENTS AND FORCES BETWEEN CHAIN AND PULLEYS

For every gear ratio the nominal operation radii and the nominal wrap angles result from the chain length and the center distance of the pairs of pulleys. In case of a gear ratio change with the adjusting-speed diV/dt, the changes of the contact radii drA/dt and drB/dt on both pulleys are different. Figures 4 and 5 clarify these relationsships.
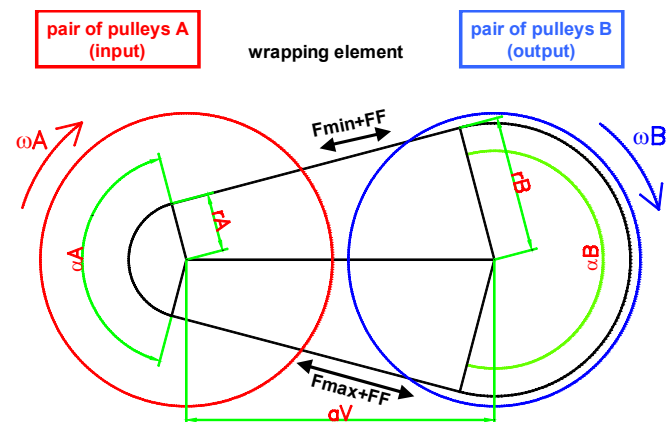

Fig. 4: Nominal radii rA und rB and nominal wrap angles αA und αB

The pulling force in this chain strand, that runs up the driving pulleys A, is called Fmax, whereas the pulling force in the other chain strand is called Fmin. On the wrap curves the chain is affected by centrifugal forces, which lead to a supplementary pulling force FF in the chain. This force FF depends on the chain speed and the chain mass per length.

$$FF = \frac{m_K}{L_K} \cdot v_K^2$$

This chain force influences the power transmission by this additional chain strain only to a very small extent. In the following, the force F refers to the total chain force minus the centrifugal force FF.
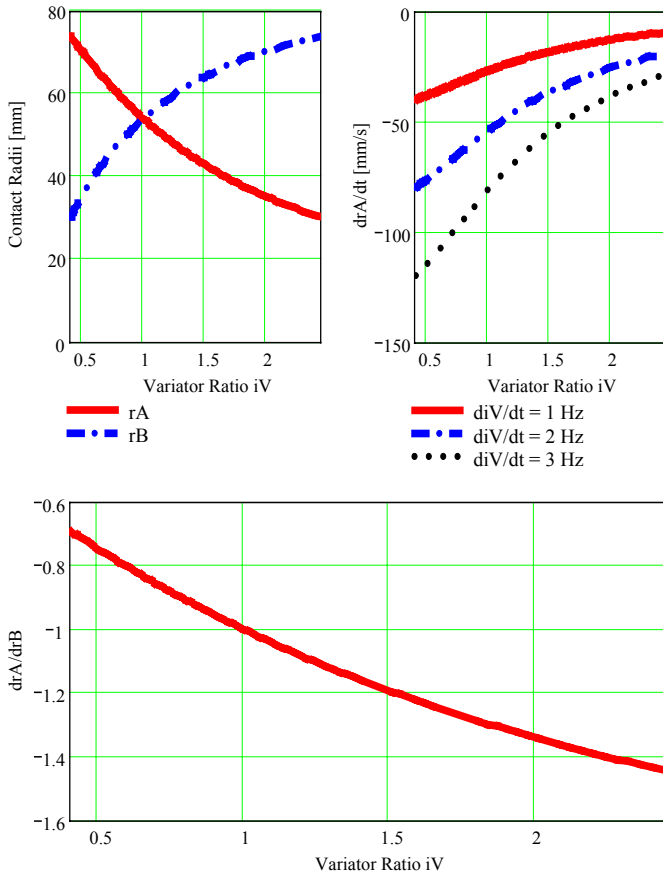

Fig. 5: Nominal radii rA und rB and their temporal change with the variator ratio iV.

The conical pulleys of the variator may have a curvature ($r_{curvature}$). In conjunction with crowned chain pins this leads to different contact areas between a pin and a pulley at different gear ratios. In consequence, the wear reduces during the gear lifetime. In addition, this pulley curvature leads to variable wedge angles of the pulleys changing with the contact radius of the chain/a pin.

Figure 6 shows a movable variator pulley, which is not deformed, and the deformation of a variator pulley loaded with a single force. From such FEM calculations results a matrix for each pulley for the calculation of the deformation at the position k with a load at the position j. Subsequently, the entire pulley deformation can be calculated from the linear overlay of all single deformations as a consequence of all contact forces between chain and pulleys.

Furthermore, the gaping of the movable pulley has to be added to these deformations. This gaping depends on the guidance length and the guidance clearance of the movable pulley and the position and direction of the total clamping force. Therefore the gaping causes a wedge angle $\beta(\alpha)$ that varies with the wrap angle α.

Taking into consideration the shortening of a chain pin by a clamping force, it is possible to compute the radial local displacement of the chain into the wedge gap.
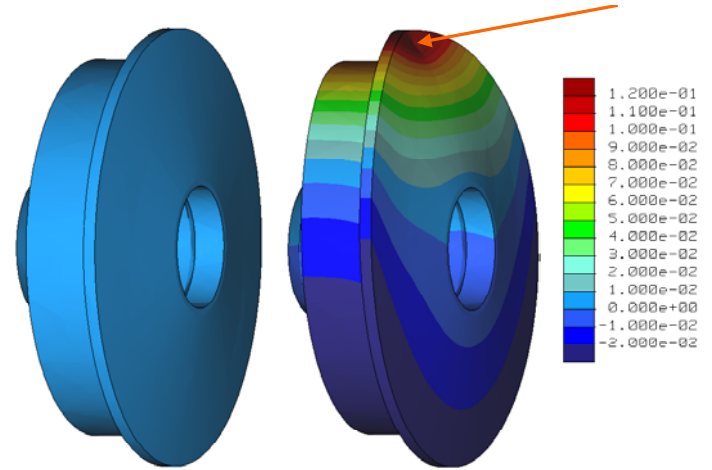

Fig. 6: Pulley deformation at load with a single force
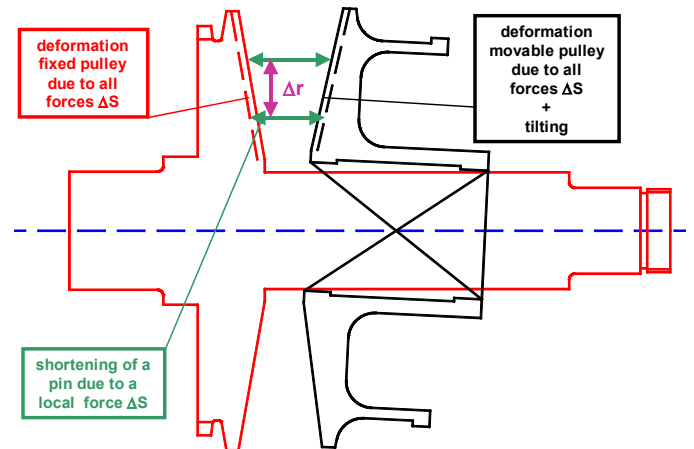

Fig. 7: Radial pin displacement due to different parts of deformation

Fig. 8 illustrates the speed conditions at a contact point between the chain and the pulleys. At the momentary operation radius the pulley has a speed vS. The chain has a speed vK changing with the total chain force (F+FF). The angle κ indicates the direction of the chain speed and depends on the small radial sliding speed due to the elastic deformations. A ratio change with a gradient of diV/dt leads to additional adjusting-speeds vv and vu, that may be relatively large at fast ratio changes. According to the law of continuity, the chain can slide only at one contact point with the speed vv=dr/dt in radial direction towards the pulleys. All other chain pins then have an additional sliding speed (vu) in circumferential direction, which increases linearly with

the absolute angle between this chain pin and the position, where the chain slides only in radial direction. The total sliding speed vKS of the chain towards the pulleys as well as the sliding angle γ results from the overlay of all these speeds.
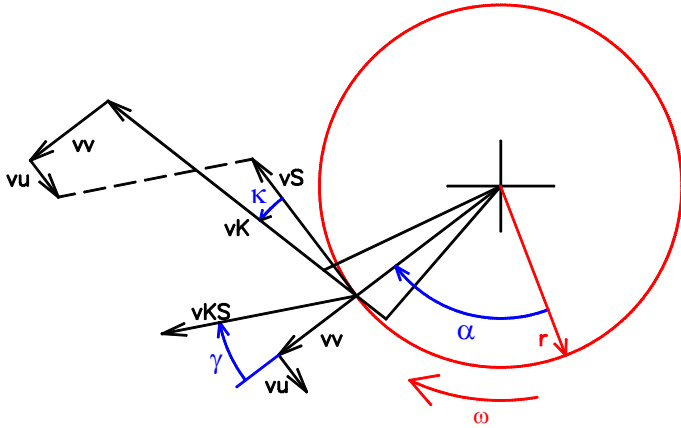

Fig. 8:   Speed conditions in a contact point between chain and pulley

Fig. 9 demonstrates the contact forces at one chain pin. The local normal force ΔN operates vertically to the pulley surface. It creates a friction force R in opposite direction of the total slip with its particular component R° in a cross section, which is perpendicular to the pulley axis. The axial components of these two forces result together in the local clamping force ΔS. The friction force R° causes the change of the tractive chain force.
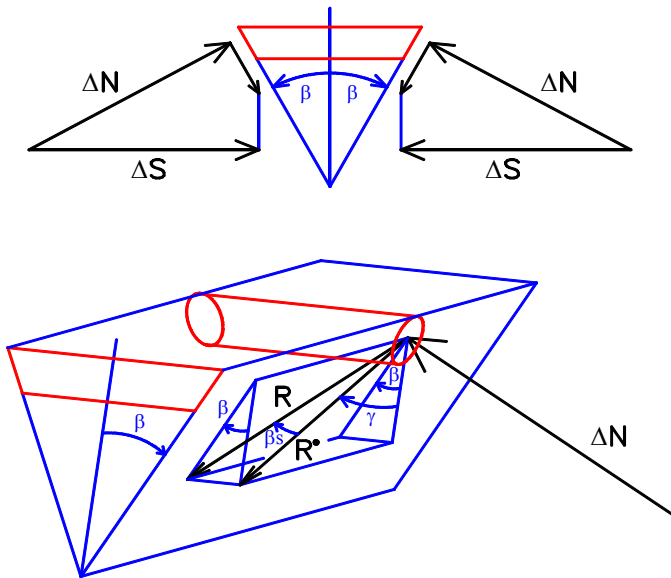

Fig. 9: Contact forces at a pin of a chain

Figure 10 shows the chain pins i-1, i, and i+1 on the wrap curve. The tractive chain forces Fi and Fi+1 pull at the pin i. The wrapping situation is characterized by the local contact radii r. Consequently, the chain pitch yields the angles $\Delta\alpha i$ and $\Delta\alpha i+1$. Thus, the equations for balanced forces can be formulated now. Then it is possible to compute both the force changes as well as

the contact loads. The following four ranges of the sliding angle γ can be distinguished for the analysis of force changes.

	decreasing chain force	increasing chain force
Radial sliding of the chain outwards the wedge gap	-0° > γ > -90°	0° < γ < 90°
Radial sliding of the chain inwards the wedge gap	-90° > γ > -180°	90° < γ < 180°

The equations to calculate the chain forces and contact forces are:

$$F_{i+1} = F_i \cdot \frac{\cos(\Delta\alpha_i) + \sin(\Delta\alpha_i) \cdot \dfrac{\mu \cdot \cos(\beta s) \cdot \sin(\gamma)}{\sin(\beta) - \mu \cdot \cos(\beta s) \cdot \cos(\gamma)}}{\cos(\Delta\alpha_{i+1}) - \sin(\Delta\alpha_{i+1}) \cdot \dfrac{\mu \cdot \cos(\beta s) \cdot \sin(\gamma)}{\sin(\beta) - \mu \cdot \cos(\beta s) \cdot \cos(\gamma)}}$$

$$\Delta N = \frac{1}{2} \cdot \frac{F_i \cdot \sin(\Delta\alpha_i) + F_{i+1} \cdot \sin(\Delta\alpha_{i+1})}{\sin(\beta) - \mu \cdot \cos(\beta s) \cdot \cos(\gamma)}$$

$$\Delta S = \Delta N \cdot (\cos(\beta) + \mu \cdot \sin(\beta s))$$

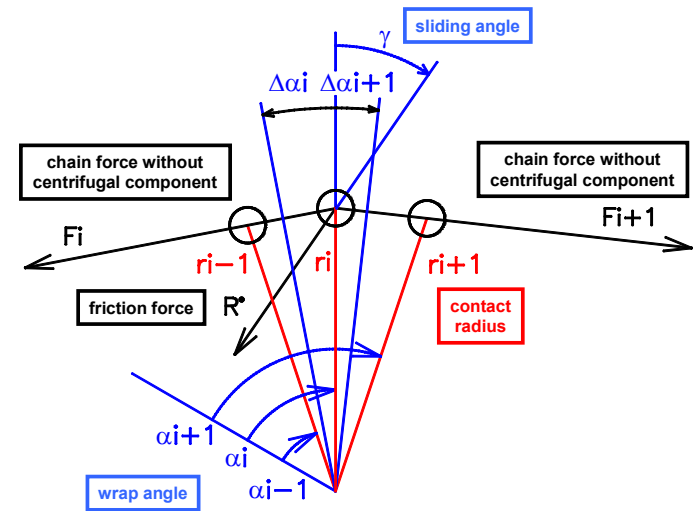$$\tan(\beta s) = \tan(\beta) \cdot \cos(\gamma)$$

Fig. 10: Change of the chain force F through the component R° of the friction force R

ALGORITHM FOR THE CALCULATION OF AN OPERATING STATE

The force change ΔF depends on the friction angle γ. On the other hand, γ depends on the sliding speed vKS that is influenced by elastic deformations at the chain and the pulleys. Moreover, these deformations depend on the chain forces and the contact forces.

Now the question for the calculation of the entire power transmission arises. How is it possible to calculate the

entire power transmission on both pulleys and the subsequent chain forces $F(\alpha)$ that depend on so many parameters ? Given inputs are the gear ratio iV and its change in time diV/dt, the rotation speed n and the torque T which is to be transmitted, e.g. at the input pulley A, and the clamping force S adjusted by the controller system, e.g. at the output pulley B.

This new calculation algorithm solves this task by means of several interlaced calculation processes. On purpose, especially CPU time consuming and numerically large-scale solutions of connected systems of differential equations are avoided.

With the gear ratio iV and the adjusting-speed diV/dt, the average operating radii rA and rB between the chain and the pulleys as well as the time gradients drA/dt and drB/dt are known. With the input of the torque TA or TB the circumferential force Fu, which has to be transmitted, is known as well. For the further calculations, in a first step the chain force and the chain speed in the strand running onwards the pulley have to be estimated. The relation ε between the two strand forces, that perhaps is known from the experience, helps to estimate the chain force quite realistically.

$$\varepsilon = \frac{Fmax}{Fmin} = \frac{Fmax}{Fmax - Fu}$$

As the first chain speed, for example, the pulley speed on the mean radius can be chosen.

A first pulley deformation can now be calculated with an estimated course of the chain forces from the force in the strand running onto the pulleys up to the force in the strand running off the pulleys. Already a simple exponential equation is sufficient here for the first course of the chain force. In addition, it is necessary to have reasonable functions of the slip angles at the pulleys A and the pulleys B, which can be estimated from experiences or former calculations.

In fact this computation algorithm would even work with a first linear force course and a constant sliding angle. However, in this case one or two additional iteration steps might be necessary until the exact solution is found.

Having estimated the pulley deformations, one gets the information about the local contact radii of the chain pins as well as the sliding speeds of the radial sliding movement inwards or outwards the wedge gap due to the elastic deformations. Together with the sliding speeds from the gear ratio change, a new curve of the sliding angle is available. Thus, the force change from the force in the on-running strand to the end of the wrap curve can now be calculated. The speed of this calculation is very high, since the force change is not being determined in infinitesimally small steps dF/dα, but from pin to pin, that is to say by a gradient $\Delta F/\Delta\alpha$. However, the necessary CPU time will rise with a smaller chain pitch respectively a larger number of chain links.
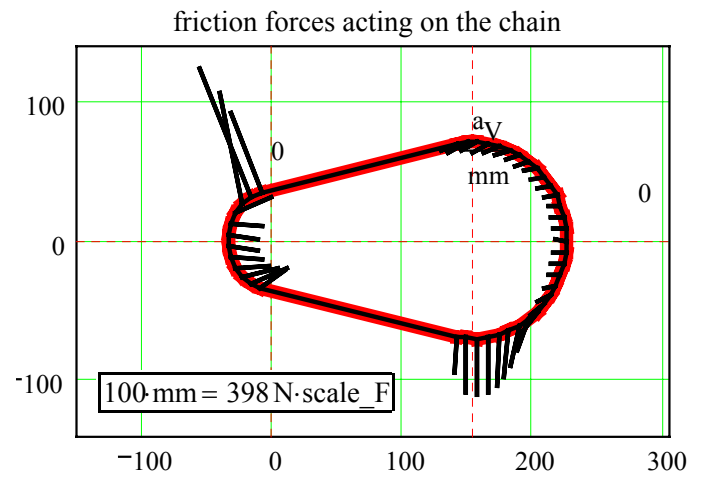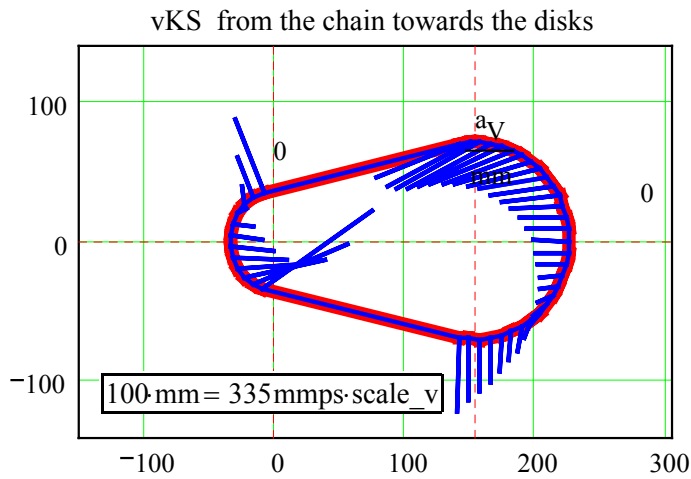
But now the force in the off-running strand does not correspond anymore with the force required from the torque-transfer. Therefore, it is necessary now to vary the chain speed in a first iterative loop until the strand force difference Fmax-Fmin corresponds to the circumferential force Fu, which has to be transmitted. If the chain speed is much larger than the pulley speed on the average radius, the sliding angle γ is almost 90° and the chain force increases significantly in wrapping direction. If the chain speed is much smaller than the pulley speed on the mean radius, the sliding angle γ comes to almost -90° and the chain force strongly decreases into wrapping direction. Between these extreme operating points there is obviously only one chain speed in the on-running strand that is exactly corresponding with the required torque transfer. The relation between the chain speed and the circum-ferential force is strongly nonlinear. Nevertheless, with a dexterous interpolation routine it is possible to find the correct solution in just a few steps.

However, the chain force course, that has been determined in this way, is still based on estimated pulley deformations. For this reason, with these new chain forces new pulley deformations are calculated now in a second iterative loop. These more accurate deforma-tions allow a more precise formulation of the chain force course. This iteration processes will be repeated until the course of the chain force does not change anymore.

The sum of the local clamping forces ΔS is the total clamping force S, which increases with the chain force in the strand that runs onto the pulleys. This chain force, up to now only estimated, can now be varied in a third iterative loop until the total clamping force S corresponds to the input from the controller. Here, the relation between S and the function $1/(\varepsilon-1)$, which is almost linear, supports a fast convergence.

In total, these three interlaced iterative loops run very fast. The CPU time rises with smaller chain pitches. It rises also with locally very smooth pulleys, because then a different distribution of the contact forces leads to significantly different deformations.

On principal, this calculation algorithm is the same for both pairs of pulleys. The first step is the calculation for that pair of pulleys, for which the clamping force S is controlled by the hydraulic system. Often this is the driven pair of pulleys B. As one result we already get both strand forces Fmax and Fmin. This is now one main input for the calculation at the other pair of pulleys. Here the third iterative loop can be omitted. The second clamping force necessary for the power transmission is also yielded from the contact loads on this second pair of pulleys. An important result of this calculation is therefore the so-called clamping ratio ζ as the relation of the clamping forces SA/SB.

vKS from the chain towards the disks

$100\,mm = 335\,mmps \cdot scale\_v$

friction forces acting on the chain

$100\,mm = 398\,N \cdot scale\_F$

stiffness = "normal"

$iV = 2$

$vK = 7.35\dfrac{m}{s}$

$r_A = 35.1\,mm$

$nA = 2000\,min^{-1}$

$r_B = 70.2\,mm$

$nB = 1001\,min^{-1}$

$diVdt = 0\dfrac{1}{s}$

$drAdt = 0\dfrac{mm}{s}$

$drBdt = 0\dfrac{mm}{s}$

$TA = 0.5\,Nm$　　$Pan = 0.1\,kW$

$Fu = 14\,N$　　$\eta_{KS} = 78.77\%$

$FF = 65\,N$　　$\mu_{max} = 0.09$

$Fmax = 723\,N$　　$PVA = 10.6\,W$

$Fmin = 709\,N$　　$PVB = 11.6\,W$

$\varepsilon = 1.02$　　$SA = 5.4\,kN$

$\zeta = 0.897$　　$SB = 6\,kN$

input A　　　　　output B

γ [°]

r-r_m [μm]

bolt-Nr. on the wrap curve

input A　　　　　output B
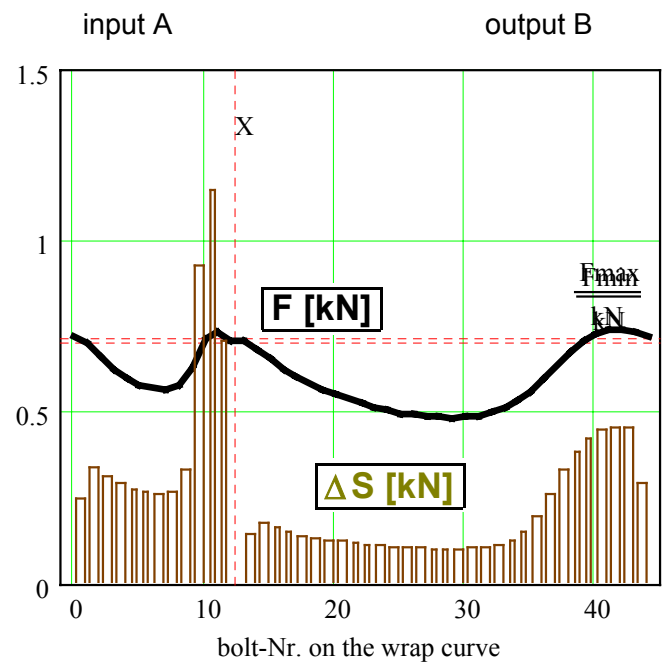

F [kN]

$\dfrac{Fmax}{kN}$

ΔS [kN]

bolt-Nr. on the wrap curve
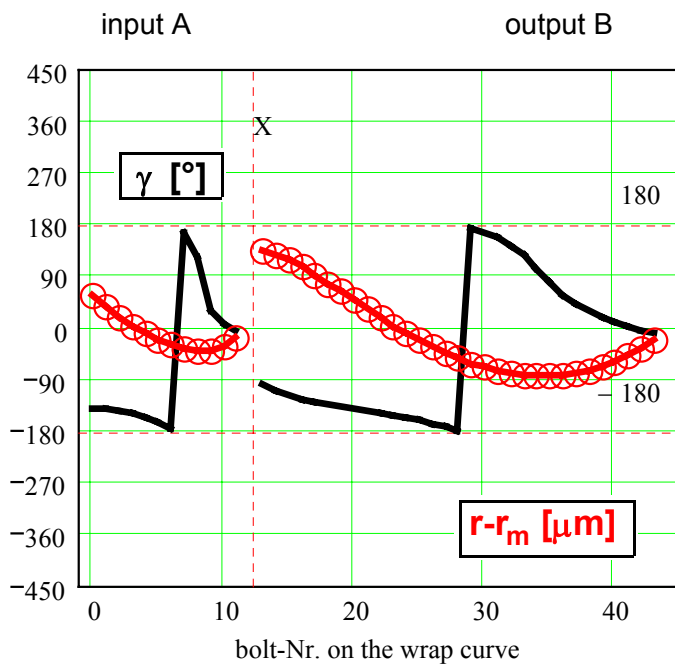
Fig. 11:　Operating point with constant ratio:

iV=2.0, diV/dt=0 Hz,
TA=0.5 Nm, nA=2000/min, ε=1.02, SB=6 kN

vKS from the chain towards the disks

$$100 \cdot mm = 335 \, mmps \cdot scale\_v$$

friction forces acting on the chain

$$100 \cdot mm = 398 \, N \cdot scale\_F$$
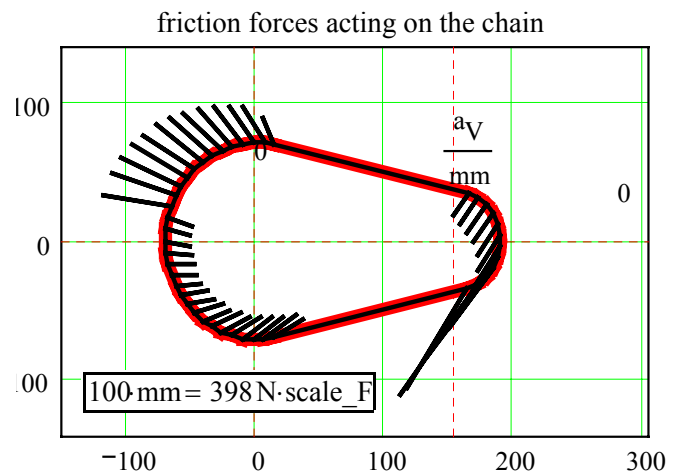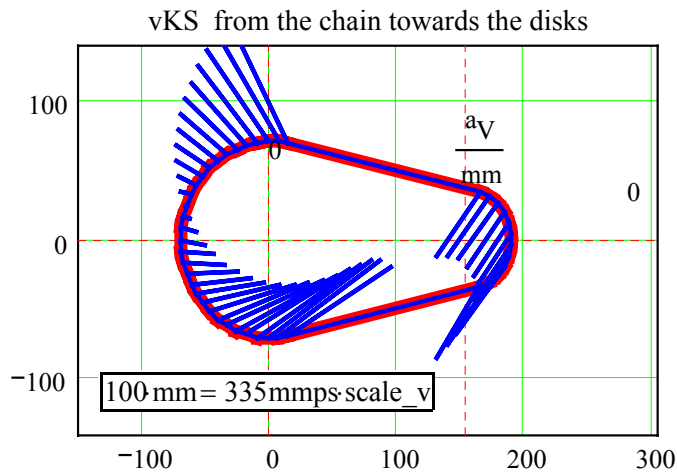
stiffness = "normal"

$iV = 0.5$	$vK = 14.72 \dfrac{m}{s}$
$r_A = 70.3 \, mm$	$nA = 2000 \, min^{-1}$
$r_B = 35.1 \, mm$	$nB = 3981 \, min^{-1}$

$$diVdt = 0 \, \frac{1}{s} \qquad drAdt = 0 \, \frac{mm}{s}$$

$$drBdt = 0 \, \frac{mm}{s}$$

$TA = 250 \, Nm$	$Pan = 52.4 \, kW$
$Fu = 3558 \, N$	$\eta_{KS} = 96.3\%$
$FF = 260 \, N$	$\mu_{max} = 0.09$
$Fmax = 6228 \, N$	$PVA = 1209.9 \, W$
$Fmin = 2670 \, N$	$PVB = 729.4 \, W$
$\varepsilon = 2.333$	$SA = 46.6 \, kN$
$\zeta = 1.726$	$SB = 27 \, kN$
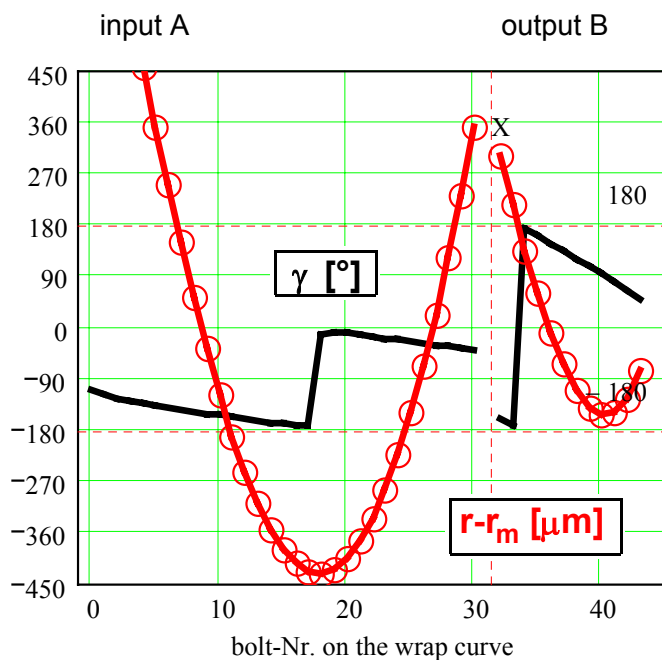
input A   output B

bolt-Nr. on the wrap curve
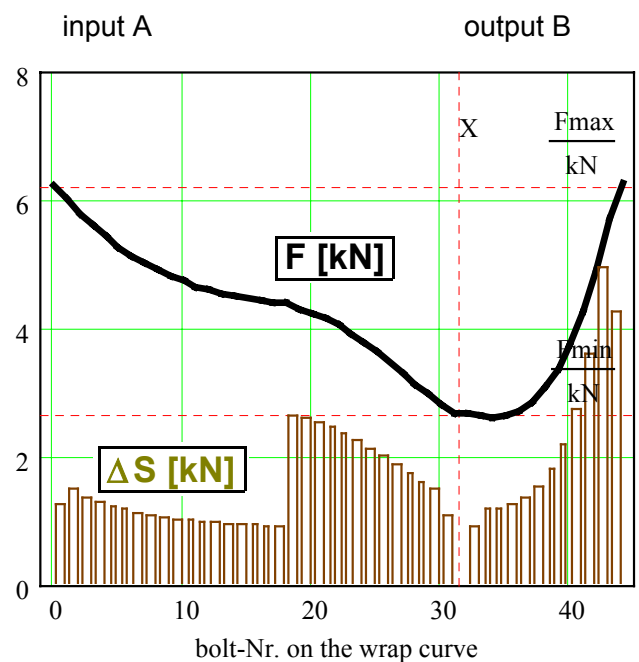
input A   output B

bolt-Nr. on the wrap curve

Fig. 12: Operating point with constant ratio:

iV=0.5, diV/dt=0 Hz,
TA=250 Nm, nA=2000/min, ε=2.331, SB=27 kN

vKS from the chain towards the disks

$$100 \cdot mm = 335\,mmps \cdot scale\_v$$

friction forces acting on the chain

$$100 \cdot mm = 398\,N \cdot scale\_F$$
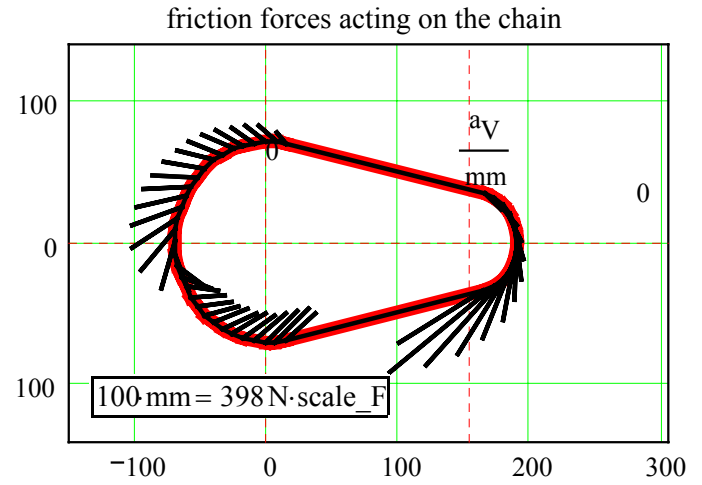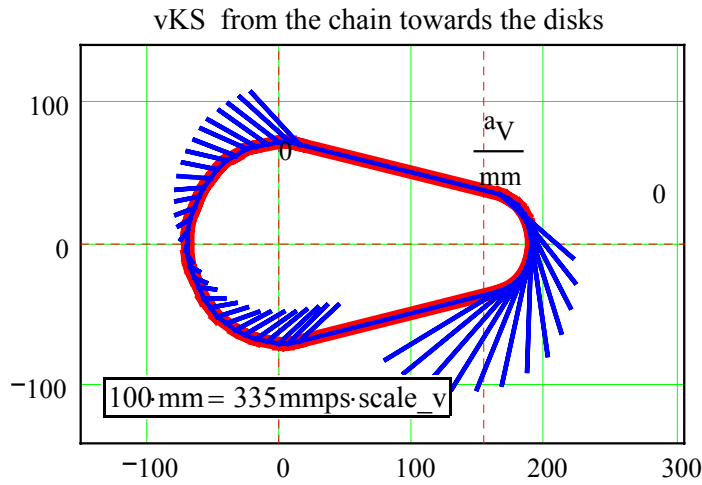
stiffness = "normal"

$iV = 0.5$ $vK = 14.72\dfrac{m}{s}$

$r_A = 70.3\,mm$ $nA = 2000\,min^{-1}$

$r_B = 35.1\,mm$ $nB = 3901\,min^{-1}$

$diVdt = 0\dfrac{1}{s}$

$drAdt = 0\dfrac{mm}{s}$

$drBdt = 0\dfrac{mm}{s}$

$TA = 250\,Nm$ $Pan = 52.4\,kW$

$Fu = 3558\,N$ $\eta_{KS} = 96.17\%$

$FF = 260\,N$ $\mu_{max} = 0.09$

$Fmax = 4744\,N$ $PVA = 548.8\,W$

$Fmin = 1186\,N$ $PVB = 1458.8\,W$

$\varepsilon = 4$ $SA = 28.4\,kN$

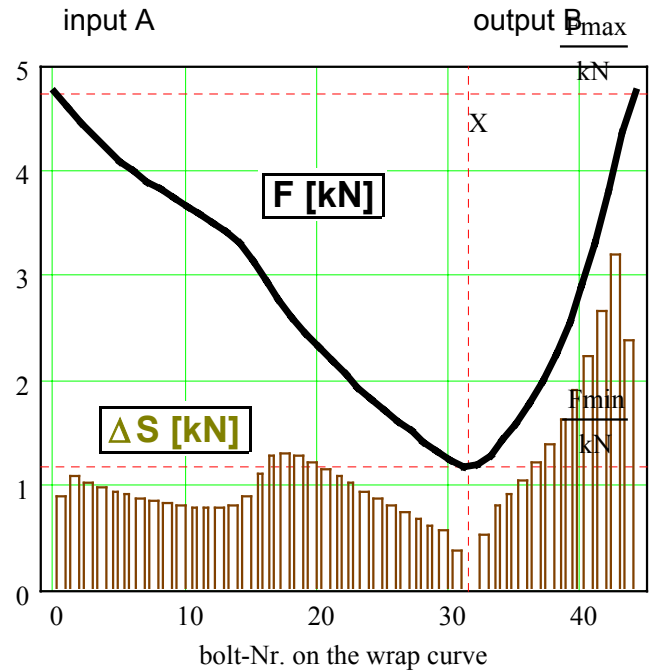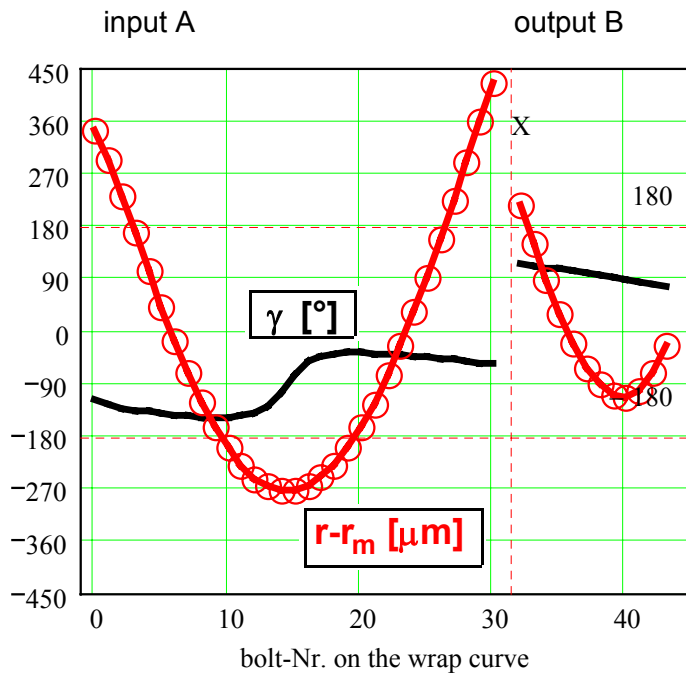$\zeta = 1.424$ $SB = 19.9\,kN$

input A — output B

input A — output B

Fig. 13:   Operating point with constant ratio:

iV=0.5, diV/dt=0 Hz,
TA=250 Nm, nA=2000/min, ε=4.000, SB=19.9 kN

Furthermore, the local power losses ∆PVA and ∆PVB can be derived from the sliding speeds between the chain pins and the pulleys and from the friction forces being effective there. The addition of the local power losses yields the total losses PVA and PVB in the contacts between the chain and the pulleys. Finally this results in the degree of efficiency ηKS of the power transmission.

CALCULATION EXAMPLES

Some exemplary calculations shall now demonstrate the performance of this new development instrument.

Figure 11 clarifies the contact situation with the constant gear ratio iV=2.0 and a very small input torque TA=0.5 Nm with a minimal clamping force at the driven pair of pulleys of SB=6 kN. Although the torque is almost 0, the chain force changes on both wrap curves. The contact pressures at the pulleys lead to disk deformations so that the chain slides first into to the wedge gap on both wrap curves and then out again. At the beginning of the wrap curve this leads to a chain force decrease. Then the sliding motion turns outwards and the chain force increases. The graphs of the sliding angles at the variously big wrap curves are similar at both pairs of pulleys. The sliding movements and friction forces cause a power loss which leads to a low degree of efficiency ηKS at a small input power.

Figure 12 shows the contact conditions at a constant gear ratio iV=0.5 and a relatively high load TA=250 Nm. On the driving pair of pulleys A close to the centre of the wrap curve the typical bend in the force graph can be seen. The reason for that is, that at this position the sliding angle γ jumps from values around -180° onto values around 0°. Thereby, the local contact forces in this area increase very strongly and with that also the friction forces increase rapidly. This leads to the change in the force gradient ∆F/∆α.

On the driven pair of pulleys B the wrapping begins with sliding angles of about 180°. That is to say that here the force changes ∆F/∆α are almost 0. In the past this range at the beginning of this wrap curve was described as a "rest curve". With increasing wrap angle the sliding angle decreases from γ=180° to γ=90°. With these sliding angles the chain slides into the wedge gap. The force change is at maximum at γ=90°. If the sliding angle is lower than 90°, the chain slides out of the wedge gap and the change of the chain force becomes smaller again.

The only difference between the operating state to Figure 3 and that to Figure 12 is the supplementary adjusting-movement diV/dt<0 towards an even smaller gear ratio. With the same strand force ratio this can be achieved by a larger clamping force SA at the driving pair of pulleys A and a smaller clamping force SB at the other pair of pulleys B. The supplementary sliding movements from changing the gear ratio overlay the

sliding movements from the elastic deformations. At the pair of pulleys A the absolute sliding movements decrease on the first part of the wrapping, where the chain moves into the wedge gap, and they increase in the range, where the chain moves outwards the wedge gap. By that the regions of inward and outward sliding do slightly change. This effect becomes visible in the changed position of the point where the sliding angle jumps from γ=-180° to γ=0°. In total, the contact forces do slightly increase. As a result, the losses increase a little at this pair of pulleys in the comparison to the stationary operating state. At the pair of pulleys B the inwards movements, that are dominating at this gear ratio, are reinforced by the negative adjusting-speed drB/dt<0. In spite of the contact forces, which are somewhat smaller, the contact losses therefore increase to some amount here. The degree of efficiency of the power transmission between chain and pulleys decreases by approximately 0,5 %. Changes of the gear ratio to underdrive with small adjusting-speeds at first even lead to an increasing of the efficiency. Only very fast adjusting-movements reduce the degree of efficiency noticeably.
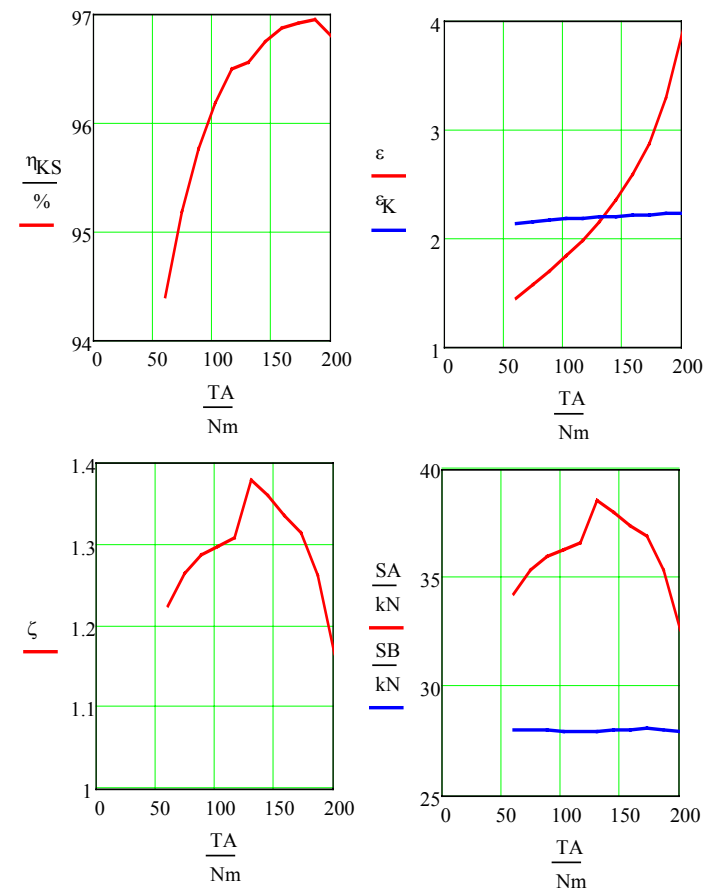

Fig. 14:   ζmax-test

Operating point: iV=1.5=constant, nA=2000/min, µ=0.09, SB=28 kN

In the operating point in Figure 13 the contact pressure SB is reduced in comparison to the operating point in

Figure 12. By that, the strand forces become smaller and the strand force ratio ε increases. In order to be able to transmit the same circumferential force Fu in this case of reduced contact pressure, bigger force gradients ΔF/Δα are necessary. At the input pulleys the course of the sliding angles approaches the limiting angle γ=-90° and at the driven pair of pulleys it approaches the limiting angle γ=90°. The "rest curve" at the driven pair of pulleys B has disappeared. A further enlargement of the torque would very soon lead to a complete circumferential slip of the chain towards the driven pulleys.

Although the clamping forces and, because of that, the contact forces are clearly lower than those in the operating state in Figure 12, the degree of efficiency ηKS is somewhat smaller. This is the result of the higher sliding speeds just before the total slip.

pair of pulleys. Such experiments are known as "ζmax-tests". With increasing input torque TA the clamping ratio ζ increases at first up to a peak value in order to fall again afterwards. The torque at ζmax is the "nominal torque" TA_nominal=135 Nm for this clamping force SB=28 kN. At this point the chain efficiency is almost at maximum and a sufficient safety from total slip exists there.

The control maps for such CVTs regarding the optimal clamping are often evaluated from those experimental ζmax-tests. Furthermore, some other maps like those for an optimal strand force relation ε_K can be determined with these ζmax-calculations. These information can be useful for further simulations regarding an optimal design for the hydraulic control system. Moreover, the power transmission can be computed even faster with knowledge of the strand force ratio ε.
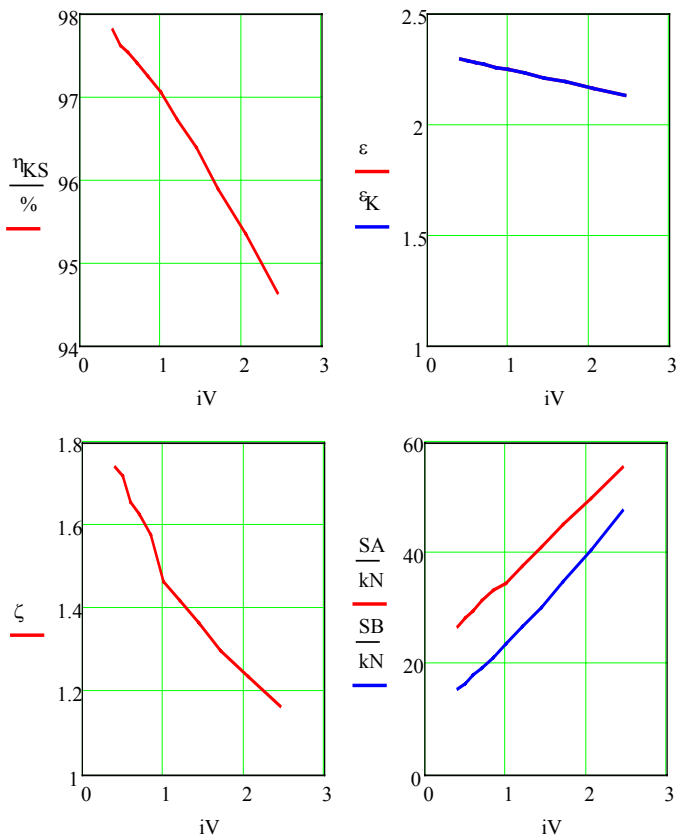

Fig. 15: Graphs of the clamping ratio, the clamping forces and the efficiency via the gear ratio iV

Operating point: TA=150 Nm, nA=2000/min, μ=0.09, diV/dt=0/s

Therefore, for every operating state there must be an optimal contact pressure at which both the safety from total slip as well as the degree of efficiency are equally good. For this exemplary gear Figure 14 shows the graph of the clamping ratio ζ=SA/SB via the input torque TA. Further parameters are the constant gear ratio of iV=1.5 and the constant clamping force SB at the driven
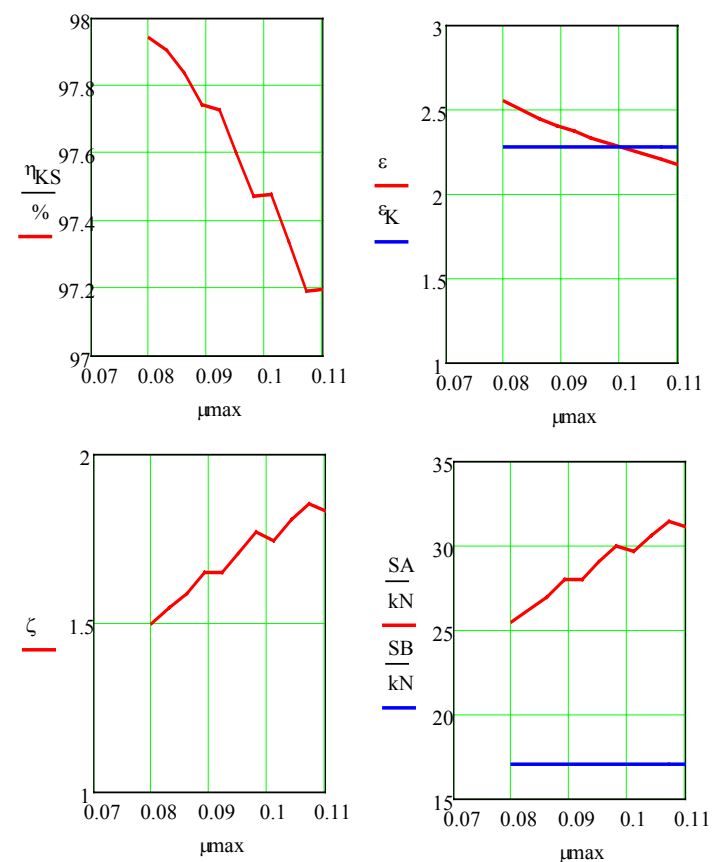
Fig. 16: Influence of the friction coefficient on clamping ratio ζ and efficiency ηKS

Operating point: iV=1.5=constant, TA=150 Nm, nA= 1000/min, ε=2.205, μ=0.09

Figure 15 shows the graph of the clamping ratio ζ for this gear via gear ratio, which is constant in each case. For this example the optimal strand force ratio $\varepsilon = \varepsilon_K$ has been determined from ζmax-calculations. Obviously, in case of a constant ratio the clamping force SA at the

input pulleys A is always higher than the clamping force SB at the output pulleys B. This is even the case in operating points with a big gear ratios iV and a small wrap curve at the input pulleys when there are little contact radii.

At the input pulleys there are far larger wrapping ranges with sliding angles around $\gamma=0°$. As a result of this the local clamping forces increase significantly. In underdrive ratio the clamping ratio ζ is only slightly bigger than 1 and increases noticeably when the ratio turns to overdrive. The high clamping forces in underdrive cause relatively large sliding movements and thereby relatively high losses. The chain efficiency rises when changing the ratio from underdrive to overdrive. These results are proven through many experiments.
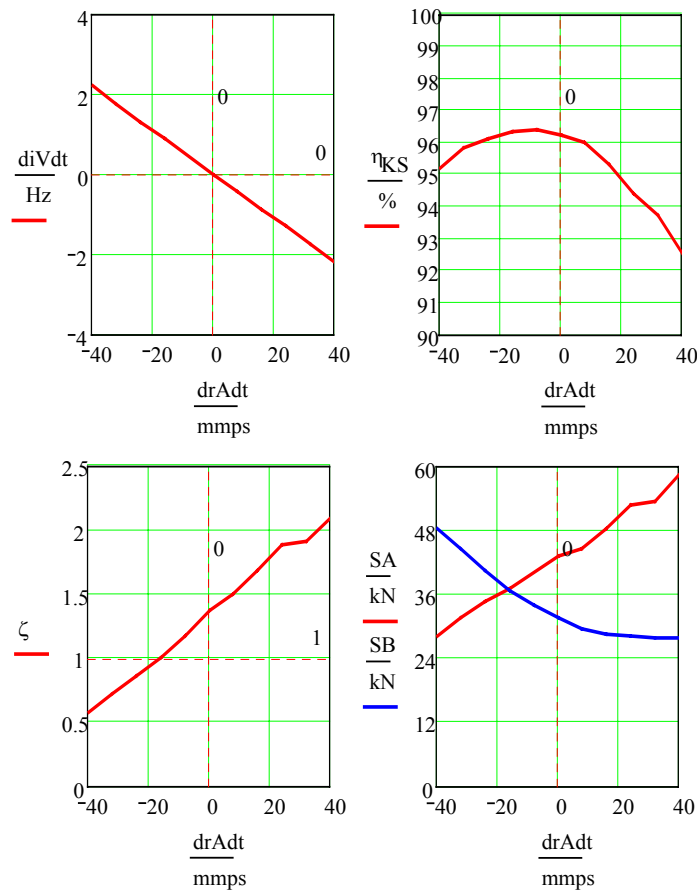

Fig. 17: Influence of the adjusting-speed drA/dt on the clamping forces SA und SB, the clamping ratio ζ and the efficiency ηKS at constant force ratio ε.

Operating point: iV=1.5, TA=150 Nm, nA= 1000/min, ε=2.205, μ=0.09

During the lifetime of a chain-CVT the pulleys and the contact surfaces of the chain pins become burnished. In general, this leads to a reduction of the friction coefficient. The calculations for Figure 16 show that the clamping ratio ζ decreases then and the strand force ratio ε as well as the chain efficiency ηKS increase

slightly. Also these results could be already confirmed by experiments.

Finally, the Figures 17 and 18 show the influence of the adjusting-speed on clamping forces, clamping ratio, and contact losses. For the calculations for Figure 17 the strand force ratio ε shall remain constant in order to have sufficient safety from total slip of the chain at any time. If then the ratio iV=nA/nB=rB/rA is changed to underdrive, it is necessary to increase the clamping force SB at the driven pair of pulleys and to reduce SA at the driving pulleys. A ratio change to overdrive requires an increasing of SA and a reduction of SB. As already mentioned above, the degree of efficiency increases slightly if the ratio is changed to underdrive comparatively slow. Only if the ratio is changed quickly, the degree of efficiency of the power transmission decreases in both adjusting-directions.
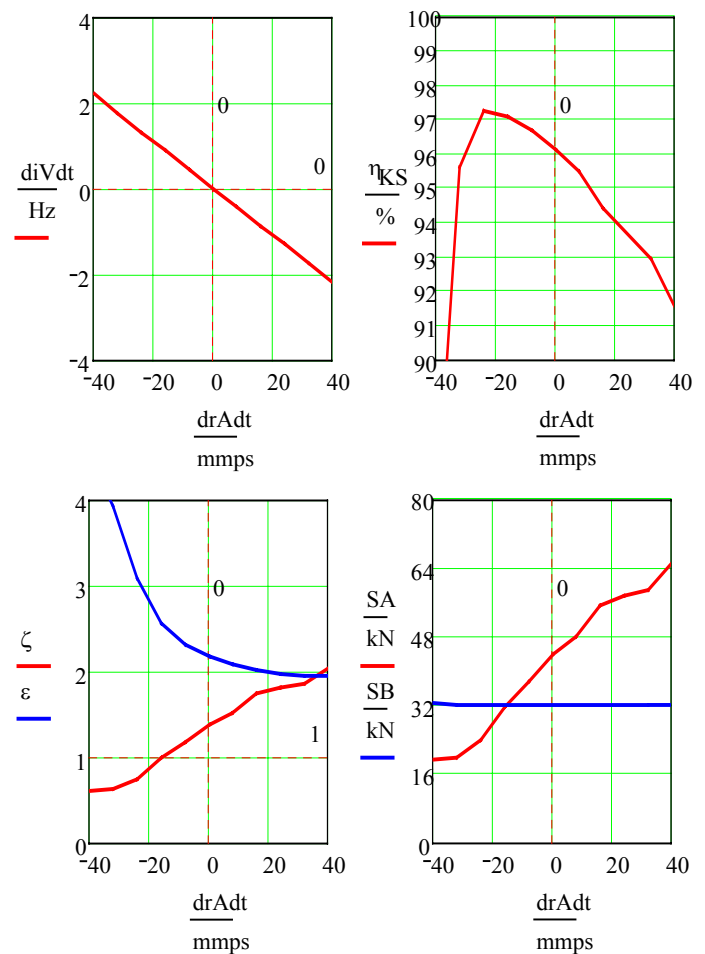

Fig. 18: Influence of the adjusting-speed drA/dt on the spread force SA, the clamping ratio ζ and the efficiency ηKS at constant spread force SB.

Operating point: iV=1.5, TA=150 Nm, nA= 1000/min, SB=32 kN, μ=0.09

For the gear ratio change to Figure 18 the clamping force SB at the driven pair of pulleys is held at a constant level. In order to reduce now the gear ratio

swiftly, SA must be further increased. The degree of efficiency falls off more steeply than with the ratio change according to Figure 17 where SB is reduced also. In order to extend the gear ratio swiftly, SA must be reduced very strongly. By that, the strand force ratio ε increases and the safety from total slip drops. Then the increased sliding movements lead also to bigger losses.

CONCLUSIONS

The power transmission in continuously variable wrapping gears is in particular a complex process, especially in operating points with variable ratio. Until today this process can hardly be described with an all-encompassing theory. Most of the computational programs that have been developed up to now are limited to stationary operating states. However, some of these programs [9] are capable to consider three-dimensional chain oscillations. All these programs solve very complex systems of equations with time-consuming algorithms. But by that these programs become slow and in part it is difficult to work with them. Therefore the aim of the research work presented here was the development of a calculation instrument, whereby the power transmission in a wrapping-CVT can be determined relatively rapid also in non-stationary operating points. Furthermore, this instrument should be easy to handle.

The computational program that was created for this purpose works with a new solution algorithm. This algorithm balances all the chain forces and the forces on the pulleys. Furthermore, it takes into consideration the relations between the elastic deformations, the ratio change, and all the various sliding speeds. Instead of the numeric integration of a connected DGL-system, the program uses several iterative loops which are nested within each other. With the information about the elasticity of the pulleys and the speed of the chain at the beginning of the wrap curve, the program computes the force change in the chain from one pin to the next. Using the additional information about the clamping force, the real local pulley deformations can be computed by iteration algorithms that converge very fast. In addition, this new program can compute all the forces on the chain and the degree of efficiency of the power transmission from the input pulleys via the chain to the output pulleys, even in operating points with dynamic ratio changes. Because the necessary clamping forces are calculable in these non-stationary operating points too, the program can support calculations for the dynamic behaviour of chain and belt-CVTs and the development of improved hydraulic control systems.

For all stationary operating points the computational program finds solutions which correspond closely with the very recent theoretical and experimental results from Sattller [7] and Sue [8]. Also the additional relations presented here between the adjusting-movements for the ratio change and the clamping forces necessary for that can be proven experimentally as well as the supplementary losses occurring in this case.

For the calculation of one operating point this new computational program needs only between 30 s and 60 s time, using a personal computer with 512 MB RAM and 3 GHz clock frequency. The calculations presented in this paper altogether required a total CPU time of less than 1 hour. In particular, because of this high computing speed this program is well suitable to analyse the influences exerted on the degree of efficiency and the necessary clamping forces by individual gear parameters like the gear geometry, the stiffnesses of the components or the friction coefficients, etc.

REFERENCES

[1] O. Dittrich, **Theorie des Umschlingungsgetriebes mit keilförmigen Reibflanken,** Diss. TH Karlsruhe, 1953.
[2] K. D. Schlums, **Untersuchungen an Umschlingungsgetrieben**, Diss. TH Braunschweig, 1959.
[3] O. Lutz, **Zur Theorie des Keilscheiben-Umschlingungsgetriebes**, Konstruktion Bd. 12, 1960.
[4] B. G. Gerbert, **Force and Slip Behaviour in V-Belt Drives**, Acta Polytechnica Scandinavica, Mech. Eng. Series No. 67, Helsinki 1972.
[5] P. Tenberge, **Wirkungsgrade von Schub- und Zuggliederketten in einstellbaren Umschlingungsgetrieben**, Diss. Ruhr-Universität Bochum, 1986.
[6] G. Sauer, **Grundlagen und Betriebsverhalten eines Zugketten-Umschlingungsgetriebes**, Diss. TU München, 1996.
[7] H. Sattler, **Stationäres Betriebsverhalten verstellbarer Metallumschlingungsgetriebe**, Diss. Uni Hannover, 1999.
[8] A. Sue, **Betriebsverhalten stufenloser Umschlingungsgetriebe unter Einfluss von Kippspiel und Verformungen**, Diss. Uni Hannover, 2003.
[9] J. Srnik, **Dynamik von CVT-Keilkettengetrieben**, VDI-Fortschrittsbericht Nr. 372 Reihe 12. Düsseldorf, VDI-Verlag 1999 / Diss. TU München, 1998.